

## DIVISION OF MORPHOGENESIS



Professor  
**UENO, Naoto**



Associate Professor  
**KINOSHITA, Noriyuki**

Assistant Professor: **TAKAHASHI, Hiroki**  
**SUZUKI, Makoto**  
 Technical Staff: **TAKAGI, Chiyo**  
 NIBB Research Fellow: **YAMAGUCHI, Takeshi**  
 Postdoctoral Fellow: **HASHIMOTO, Masakazu**  
**NEGISHI, Takefumi**  
**SUZUKI, Miho**  
**HARA, Yusuke**  
 PRESTO Researcher: **SUZUKI, Miho\***  
 SOKENDAI Graduate Student: **HARA, Yusuke\***  
**MIYAGI, Asuka**  
**HAYASHI, Kentaro**  
 Visiting Undergraduate: **TOMINAGA, Hitoshi**  
 Technical Assistant: **YAMAMOTO, Takamasa**  
**MURAKAMI, Michiyo**  
**SUZUKI, Atsuko**  
**WATANABE, Mika**  
**IIDUKA, Aya**  
 Secretary: **MIYAKE, Satoko**  
**TSUGE, Toyoko**

The complex morphogenesis of organisms is achieved by dynamic rearrangements of tissues during embryogenesis, in which change in cellular morphology as well as orchestrated cell movements are involved. For cells to know how they should change their shape and where they should move, information called “cell polarity” is essential. How then is the cell polarity established within cells? Is it intrinsically formed within the cells or triggered by extracellular cues? Furthermore, little is known as to how coordinated and complex cell movements are controlled in time and space. We attempt to understand the mechanisms underlying these events using several model animals, including frogs, fish, mice and ascidians, taking physical parameters such as force in consideration, in addition to conventional molecular and cellular biology.

### I. Biological significance of force for morphogenesis

Physical forces are a non-negligible environmental factor that can guide the morphogenesis of organisms. Such forces are generated by tissue-tissue interactions during early development where drastic tissue remodeling occurs. One good example is neural tube formation. In vertebrates, the neural tube is the primordial organ of the central nervous system and is formed by the bending of the neural plate that is a flat sheet of neuroepithelial cells. The tissue remodeling is driven by cellular morphogenesis in which selected cells in the neural plate change their shapes from cuboidal to an elongated wedge-like shape, generating a force for the tissue-bending. Recent studies have revealed that this cell shape change is controlled by cytoskeletal dynamics, namely the remodeling of F-actin and microtubules (Suzuki, M. *et al.* Dev. Growth Differ., 2012). We are currently investigating how the cellular morphogenesis is spatiotemporally

controlled.

Another example is the axial mesoderm, which elongates along the anterior-posterior axis during gastrulation cell movements by which rearrangements of the three germ layers is driven. The axial mesoderm is led by the anteriorly precedent tissue leading edge mesoderm (LEM). When surgically isolated the LEM migrates fairly rapidly toward the predetermined anterior side, while the following axial mesoderm shows little directed tissue migration. We hypothesized that the LEM generates a pulling force on the following axial mesoderm (AM). We measured the force generated by LEM and estimated it to be approximately 40 nN and confirmed by laser ablation experiments that LEM generates tension on AM (Figure 1). We concluded that the anterior movement associated with the force generation is essential for proper notochord formation (Hara, Y. *et al.* Dev. Biol., 2013).

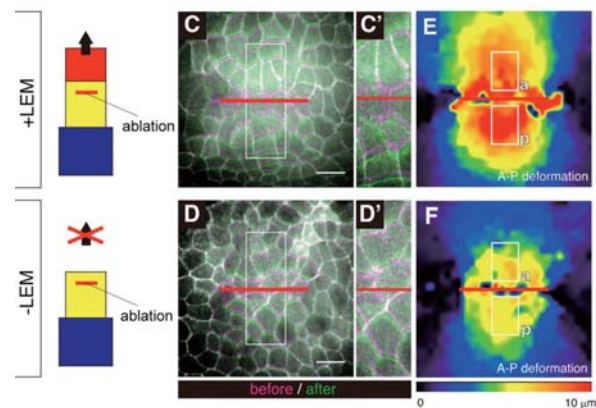


Figure 1. Laser ablation of dorsal mesoderm with and without LEM. Deformation map indicates that more significant displacement in AM after laser cutting of the tissue with LEM (upper panels, E) than without LEM (lower panels, F). From Hara, Y. *et al.*, 2013.

### II. The roles of PCP core components in mouse development

In epithelia, the roles of planar cell polarity (PCP) have been extensively studied, whereas in non-epithelia, they have yet to be fully understood. We are exploring the roles of PCP in the mesenchymal and neural tissues by using mouse genetics and RNAi knock-down technology

Recently, we generated a hypomorphic allele of mouse *Prickle1*, one of the core PCP factors. As we have reported (Tao, H. *et al.* Proc. Natl. Acad. Sci., USA, 2009) *Prickle1* null/null mice die around E6.0 in gestation due to the failure of gastrulation. In contrast, *Prickle1* hypomorphic mutant mice survive to P0. Interestingly, the mutant mice had shortened noses. Detailed analyses at the cell level suggested that PCP signaling involving core components such as *Prickle* governs convergent extension of nasal cartilage cells which is required for the lengthening of the nose. Our finding further suggests that PCP signaling employed multiple times at different places during development may be one of the universal mechanisms of organ morphogenesis. We hope that in combination with comparative genomic analysis, these

Note: Those members appearing in the above list twice under different titles are members whose title changed during 2013. The former title is indicated by an asterisk (\*).

PCP mutant mice will serve as good models that can explain morphological variations of mammals.

### III. Regulation of FGF-2 secretion and localization

Protein secretion is a fundamental process for every organism. Most of the secreted proteins have a signal peptide at the amino-terminal region. Proteins with the signal peptide are secreted through a conventional secretory pathway including ER and Golgi apparatus. Recently, however, a growing number of proteins have been found to be secreted not through the conventional ER-Golgi pathway. Those include some of the FGF (fibroblast growth factor) family members such as FGF-2. It is known that despite the lack of signal sequences, they are still secreted and play important biological roles as extracellular ligands. It is not fully understood how FGFs lacking signal peptides are secreted. In order to clarify the secretory mechanism of such proteins, we are taking a biochemical approach and performing microscopic analysis. We searched for proteins that interact with FGF-2 in the cytoplasm by mass spectrometry analysis. So far, several proteins that interact with FGF-2 have been identified. Interestingly, some of them are probably secreted through an unconventional secretory pathway as well as FGF-2. These proteins, thus, may be involved in the regulation of FGF-2 secretion. In addition, we observed the localization of secreted FGF-2 in the *Xenopus* embryonic cells (Figure 2). FGF-2 forms dots on the cell surface, suggesting that it associates with certain cell surface structures. This localization may be related to its secretion mechanism, or FGF signaling through binding with the FGF receptor. This study will contribute to clarifying a novel regulatory system for the FGF signaling pathway.

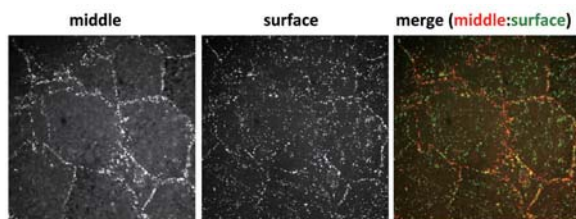


Figure 2. The localization of FGF-2 on the cell surface of *Xenopus* embryonic cells. mRNA encoding Flag-tagged FGF-2 is injected into embryos. The explant was excised from the animal pole region and FGF-2 was detected by immunofluorescence using laser scanning confocal microscopy. “middle” and “surface” indicate the focal planes of each image. In the merged image, the middle image was colored in red, and the surface image was colored in green. FGF-2 forms dot-like structures on the cell surface.

### IV. Cellular morphogenesis during neural tube closure

For the morphogenesis of organs, cellular morphogenesis as well as cellular behaviors plays critical roles. During early development of the central nervous system (CNS) in vertebrates, the neuroepithelial cells undergo a typical shape change, called apical constriction (AC), the cumulative action of which causes the neural plate to bend to form the

neural tube. In AC, cell apices are contracted and stabilized, causing cells to adopt wedge-like shapes from columnar ones. Recent studies have revealed that AC is controlled by cytoskeletal dynamics, namely the remodeling of F-actin, and non-muscle myosin II activity, yet how AC is dynamically controlled in time and space is not fully understood.

We found that during *Xenopus* neural tube closure intracellular calcium ion ( $\text{Ca}^{2+}$ ) dynamically fluctuates throughout the neural plate at single-cell to whole-tissue levels. Spatio-temporal patterns of the  $\text{Ca}^{2+}$  fluctuations appeared to be differentially regulated by the membrane-bound  $\text{Ca}^{2+}$  channel, inositol triphosphate receptor, and the extracellular signals.  $\text{Ca}^{2+}$  fluctuations temporally preceded the repeated acceleration of the closing movements.  $\text{Ca}^{2+}$  fluctuations correlated with apical constriction at the single cell level, and manipulation of cytoplasmic  $\text{Ca}^{2+}$  caused cell shape change similar to apical constriction through actomyosin contractility. These data suggest that intracellular  $\text{Ca}^{2+}$  is a positive regulator of apical constriction. We propose a dynamic  $\text{Ca}^{2+}$ -dependent mechanism and a Rho/ROCK-dependent mechanism coordinately control apical constriction in order to enable embryos to ensure the primitive central nervous system formation.

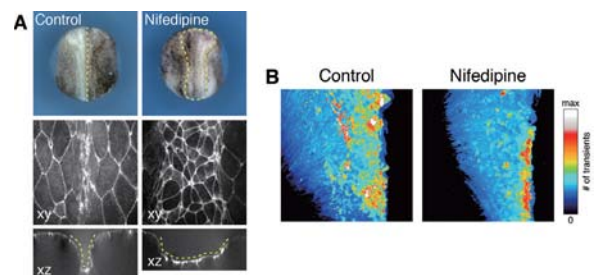


Figure 3.  $\text{Ca}^{2+}$  fluctuation is required for *Xenopus* neural tube closure. (A) Inhibition of  $\text{Ca}^{2+}$  signaling delayed neural tube closure (right). F-actin staining (middle, bottom) showed the failure of apical constriction and formation of the neural folds. (B) Intracellular  $\text{Ca}^{2+}$  patterns visualized by  $\text{Ca}^{2+}$  probe. The inhibitor treatment reduced total number of  $\text{Ca}^{2+}$  transients in the neural plate.

### V. Notochord and evolution of chordates

Amphioxus occupy a key phylogenetic position for deciphering the origin and evolution of chordates. While they develop well-organized somites, their neural tubes lack a brain-like structure; hence, they are considered acriate. Their notochords contain myofibrils. In order to characterize these three tissues of adult amphioxus, we examined their differential gene expression profiles by RNA-seq analysis. There were 1,018, 1,079, and 737 genes that were highly expressed in the notochord, somite muscle, and neural tube, respectively. Of the genes expressed in the notochord and muscle, 564 (55% of notochord genes and 52% of muscle genes) were shared, suggesting a molecular affinity between the two. On the other hand, only 119 and 104 neural tube genes were shared with notochord and somite muscle, respectively, indicating independence of genes expressed in

the neural tube. GO annotation analyses showed that genes associated with extracellular components are preferentially found in the notochord. Those associated with organelles are found in somite muscle, and those involved in synapsis and those that encode molecular transducers appear in the neural tube. The present repertoire of genes provide a molecular basis for future evo-devo studies of early chordate evolution.

## VI. Epigenetic diversification associated with subfunctionalization of duplicated genes

Polyploid organisms offer a model for understanding the evolutionary effects of gene duplication. The African clawed frog *Xenopus laevis* has experienced recent allopolyploidization, which gave rise to the pseudotetraploid genome. We found that the duplicated MyoD genes (MyoDa and MyoDb) are subfunctionalized; complementarily decreasing in the expression levels of each gene in different developmental stages, and this set of genes play roles corresponding to those of the unduplicated *Xenopus tropicalis* MyoD. To reveal the mechanisms that make MyoDa and MyoDb genes subfunctionalized, genetic and epigenetic differences between MyoDa and MyoDb were investigated. A nucleotide sequence comparison showed that MyoDa and MyoDb are 87% identical in amino acid coding regions, 5' UTR and 3' UTR. In contrast, the first intron is relatively diverged (73% identical), especially with a CpG depletion in MyoDa. We then measured DNA methylation levels in the first intron, as DNA methylation is a well-known cause of CpG depletion by deamination mutations. By means of bisulfite sequencing, we showed epigenetic differences between the duplicated MyoDa and MyoDb. The first intron of MyoDa is highly methylated, instead that of MyoDb is completely unmethylated. The constant DNA methylation levels in early developmental stages irrespective of gene activity indicated that DNA methylation is not a direct regulator. Alternatively, DNA methylation in the first intron may primarily regulate the accessibility of polycomb proteins and addition of silencing epigenetic mark trimethylated histone H3 Lysine 27 (H3K27me3), which exclusively appears on DNA methylation free regions.

### [Review articles]

- Hashimoto, M., Morita, H., and Ueno, N. (2013). Molecular and cellular mechanisms of development underlying congenital diseases. *Congenital Anomalies* 54, 1-7.
- Takagi, C., Sakamaki, K., Morita, H., Hara, Y., Suzuki, M., Kinoshita, N., and Ueno, N. (2013). Transgenic *Xenopus laevis* for live imaging in cell and developmental biology. *Dev. Growth Differ.* 55, 422-433.

### Publication List

#### [Original papers]

- Hara, Y., Nagayama, K., Yamamoto, T.S., Matsumoto, T., Suzuki, M., and Ueno, N. (2013). Directional migration of leading-edge mesoderm generates physical forces: Implication in *Xenopus* notochord formation during gastrulation. *Dev. Biol.* 382, 482-495.
- Paemka, L., Mahajan, V.B., Skeie, J.M., Sowers, L.P., Ehaideb, S.N., Gonzalez-Alegre, P., Sasaoka, T., Tao, H., Miyagi, A., Ueno, N., Takao, K., Miyakawa, T., Wu, S., Darbro, B.W., Ferguson, P.J., Pieper, A.A., Britt, J.K., Wemmie, J.A., Rudd, D.S., Wassink, T., El-Shanti, H., Mefford, H.C., Carvill, G.L., Manak, J.R., and Bassuk, A.G. (2013). PRICKLE1 interaction with SYNAPSIN I reveals a role in autism spectrum disorders. *PLoS One* 8, e80737.
- Suzuki, M.M., Yoshinari, A., Obara, M., Takuno, S., Shigenobu, S., Sasakura, Y., Kerr, A.R., Webb, S., Bird, A., and Nakayama, A. (2013). Identical sets of methylated and nonmethylated genes in *Ciona intestinalis* sperm and muscle cells. *Epigenetics Chromatin* 6, 38.
- Uno, Y., Nishida, C., Takagi, C., Ueno, N., and Matsuda, Y. (2013). Homoeologous chromosomes of *Xenopus laevis* are highly conserved after whole-genome duplication. *Heredity* 111, 430-436.